Available online at www.sciencedirect.com
SCIENCE DIRECT®
Carbohydrate Research 340 (2005) 881–887
Carbohydrate RESEARCH

Influence of homologous disaccharides on the hydrogen-bond network of water: complementary Raman scattering experiments and molecular dynamics simulations

Adrien Lerbret,* Patrice Bordat, Frédéric Affouard, Yannic Guinet, Alain Hédoux, Laurent Paccou, Dominique Prévost and Marc Descamps

Laboratoire de Dynamique et Structure des Matériaux Moléculaires, CNRS UMR 8024, Université Lille I, 59655 Villeneuve d'Ascq Cedex, France

Received 13 October 2004; accepted 28 January 2005

Dedicated to Professor David A. Brant

Abstract—A comparative investigation of trehalose, sucrose, and maltose in water solution has been performed using Raman scattering experiments and Molecular Dynamics simulations. From the analysis of the O–H stretching region in the [2500, 4000] cm^{-1} Raman spectral range, which includes for the first time the contribution of 'free' water, and the statistical distribution of water HB probabilities from MD simulations, this study confirms the privileged interaction of trehalose with water above a peculiar threshold weight concentration of about 30%. The role of the hydration number of sugars—found higher for trehalose—on the destructuring effect of the water hydrogen bond network is also addressed. The analysis of the water O–H–O bending spectral range [1500, 1800] cm^{-1} reveals a change of the homogeneity of water molecules influenced by sugars, but the three investigated sugars are found to behave similarly.

Keywords: Raman scattering; Molecular dynamics; Trehalose–water system; Sucrose; Maltose

1. Introduction

Sugars are often used in pharmaceutical, food, and biomedical applications to prepare glassy matrices for long-term storage of biological materials.[1] In recent years, the disaccharide trehalose, which is naturally produced by several organisms that are able to survive severe external stresses (temperature changes and/or dehydration), has received considerable attention. Several hypotheses have been suggested to explain the superior effectiveness of trehalose. Some of them involve direct biosystem–sugar interactions such as the 'water-replacement' hypothesis proposed by Crowe et al.,[2] which assumes that sugars hydrogen-bond (HB) to biomolecules during dehydration or freeze-drying, acting as substitutes of hydration water molecules. During this process, trehalose should be able to replace more water molecules than the other sugars. Alternative scenarios have been proposed in which some specific physical properties of sugar–water solutions are responsible for the bioprotective capability. As suggested by Green and Angell,[3] the vitrification of the sugar–water solutions should be at the origin of the inhibition of biomolecule motions. Trehalose possesses one of the highest glass transition temperatures $T_g \approx 120$ °C among bioprotecting sugars.[4,5] It has also been found as one of the most efficient ice inhibitor owing to its greater 'destructuring effect' on the water tetrahedral HB network (HBN) as emphasized by Magazù and co-workers.[6,7] Recently, Cesàro and co-workers[8] and other authors[9,10] referred to the possible role of

* Corresponding author. Tel.: +33 03 2043 4335; e-mail: lerbret@cyano.univ-lille1.fr

0008-6215/$ - see front matter © 2005 Elsevier Ltd. All rights reserved.
doi:10.1016/j.carres.2005.01.036

the polymorphic forms of trehalose in the anhydrobiosis phenomena and particularly to the reversible transformation of trehalose into a non-biodestructive anhydrous state (α phase) during water removal.

However, none of these assumptions is fully satisfactory regarding the numerous experiments (see 11 and references within) as well as numerical simulations.[12–17] For example, the water molecules replacement by sugar molecules seems reasonable for water-binding sites at the surface of a protein but not inside the protein structure. The high glass-transition temperature of sugars is certainly a pertinent parameter, but some lower-T_g systems such as trehalose–glycerol mixtures[18] are found to be better protectants. In order to better understand the physical properties of sugars in the framework of the biopreservation problem, we have performed a comparative study of three homologous disaccharides—trehalose, sucrose, and maltose—in aqueous solutions from complementary Raman scattering experiments and Molecular Dynamics (MD) investigations. We have especially focused our study on the influence of disaccharides on the HBN of water. The HB capabilities of these three sugars are directly comparable since they possess the same chemical formula $C_{12}H_{22}O_{11}$ and the same number of hydroxyl groups. Besides, it is widely accepted that Raman scattering spectroscopy is a well-suited experimental technique to accurately probe hydrogen bond networks.

2. Experiments and details of the MD simulation

High-purity maltose monohydrate, sucrose, and trehalose dihydrate were supplied from Fluka. Measurements were performed on disaccharide aqueous solutions at different weight fractions of sugar. Sucrose aqueous solutions were analyzed for sugar content from 5% to 60%, while maltose and trehalose content in disaccharide–water solutions was limited to 50% to obtain homogeneous mixtures. The mixtures were loaded in 10×5 mm quartz cells. The 514.5 nm line of a mixed argon-krypton laser was used for Raman excitation. The back-scattering Raman spectra were recorded using a Dilor-XY spectrometer equipped with a liquid nitrogen cooled charge-coupled-device detector. Spectrometer slits were kept at 300 μm, which gives a resolution-limited width of 2.5 cm^{-1} in the 2500–4000 cm^{-1} range. The 5–4000 cm^{-1} frequency range was systematically investigated at 295 K.

MD simulations have been carried out with the molecular dynamics package DL_POLY[19] on a system composed of 512 water molecules and 0, 1, 5, 13, 26, or 52 sugar molecules (either trehalose, sucrose, or maltose) corresponding to weight concentrations of 0%, 4%, 16%, 33%, 49%, or 66%, respectively. Crystallographic disaccharide conformations obtained from neutron and X-ray studies have been used in the initial configurations.[20–22] The investigated temperatures ranged from 273 to 373 K in steps of 20 K. Electrostatic interactions were handled by the reaction-field method[23] (with $\varepsilon_{RF} = 72$). We worked in the NPT statistical ensemble (the pressure was set to 1.0 bar). The time step is 0.5 fs for mixed solutions and 2 fs for pure water, and the cut-off radius is 10 Å. Cubic periodic boundary conditions have been applied. Simulations and equilibration times for the simulations at $T = 293$ K are summarized in Table 1. The Ha et al. force field[24] for disaccharides and the SPC/E model[25] for water have been used. In order to compute the density of states of water in the bending spectral range [1500, 1800] cm^{-1} for pure water and for the 49 wt % sugar–water solutions, a flexible SPC model of water developed by Teleman et al.[26] has been employed. Simulations between 500 ps and 1 ns have first been carried out at 273 K to equilibrate initial configurations. Next, short simulations of 10 ps, during which atomic velocities were stored, have been performed to compute the mass-weighted velocity autocorrelation functions of the solutions. The corresponding power spectra were then calculated to get the vibrational densities of states.

Table 1. System compositions and equilibration/simulation times at $T = 293$ K for the different sugar concentrations ϕ

ϕ (wt %)	No. sugars/no. H_2O	Eq./Sim. time (ns)		
		T	M	S
0	0/512	0.1/0.3	0.1/0.3	0.1/0.3
4	1/512	0.1/0.4	0.1/0.4	0.1/0.4
16	5/512	0.1/0.4	0.1/0.2	0.05/0.15
33	13/512	0.1/0.4	0.15/0.35	0.125/0.375
49	26/512	0.2/0.8	0.3/0.7	0.125/0.375
66	52/512	0.25/1.75	0.5/1.0	0.25/1.75

Data corresponding to $\phi = 0$ wt % result from only one simulation of pure water.

3. Analysis of the O–H–O bending mode of water molecules

This analysis gives direct information on the structural changes induced by disaccharides because there is no overlap between Raman bands of water and sugars in the bending region. However, as observed in Figure 1, the bending mode is very broad and weak. The Raman line shape in the bending region—[1500, 1800] cm^{-1}—was systematically fitted with a lorentzian function for each aqueous solution. The frequency and the half width at half maximum (HWHM) determined by the fitting procedure are reported in Table 2. An identical procedure was used in order to extract both parameters from MD calculations performed on a flexible water model. These values are compared with those obtained on pure water. Table 2 clearly shows that sugars have a weak

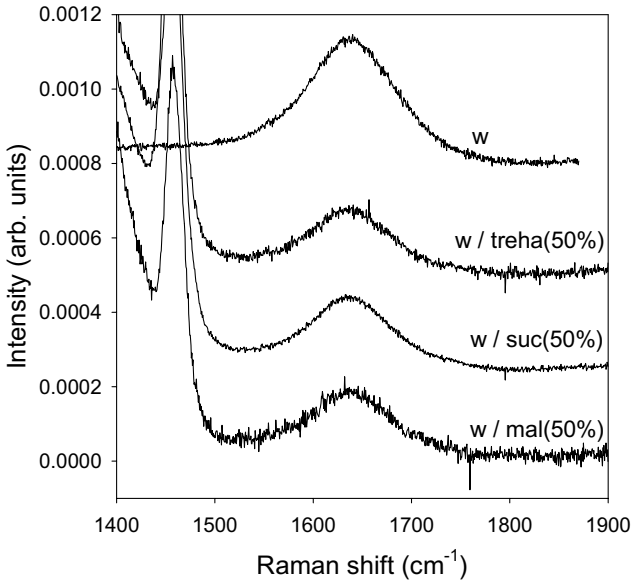

Figure 1. Raman bending mode in water and water–disaccharide mixtures with sugar weight fraction of 50%.

influence on the frequency of the δ(HOH) bending band. The frequency of this band in sugar–water mixtures is very close to that determined in pure water and does not change by increasing the content in mixtures above 30%. It can be noted that from Raman scattering experiment the frequency of the bending band in trehalose aqueous solutions is slightly downshifted with respect to that determined in water, while the opposite behavior is observed in sucrose–water mixtures. From MD calculations, this band is upshifted for the three sugars but the smallest shift is found for trehalose. Owing to the wide width of this band and the large uncertainties, it is not clear if this behavior is really significant and the authors have no clear explanation. However, both from experiments and simulations, it can be clearly observed in Table 2 that the width of the broad frequency distribution of the H–O–H bending vibrations decreases when increasing the sugar content. This general trend could be related to the presence of more homogeneous and smaller domains of water molecules influenced by the presence of sugars. No significant difference between trehalose, sucrose and maltose can be extracted from the concentration dependence of this width. Furthermore, Maréchal[27] has observed that the bulk water bending band becomes narrower with increasing temperature. This could reveal a correlation between the sharpening of the bending band and the destruction of the HBN of water. Therefore, the observed decrease of the HWHM of the H–O–H bending vibrations when adding sugars to water may indicate a similar counterintuitive behavior. In other words, this would imply that the sugars have an effect on water similar to a temperature increase. Consequently, the sugars would depress the crystallization temperature of water, thus hindering the formation of ice—and the related stresses—in living systems exposed to sub-zero temperatures. This may highlight the cryoprotective effect of sugars.

4. Water HB network

4.1. Analysis of the 2500–4000 cm^{-1} Raman spectral range

The Raman spectra of water–sugar mixtures (for 5% and 50% of sugar) recorded in the 2500–4000 cm^{-1} frequency range are reported in Figures 2 and 3. The isotropic scattering intensities were calculated from the relation $I_{iso} = I_{VV} - 4/3I_{VH}$. Each spectrum is composed of the C–H stretching modes lying between 2600 and 3100 cm^{-1}, and the O–H stretching bands in the 2800–3800 cm^{-1} frequency range, as can be observed for pure water (see Fig. 4). It is readily observed in Figures 3 and 4 that the two types of stretching bands overlap. Consequently, the whole spectrum ([2500, 4000] cm^{-1}) was fitted to determine rigorously the contribution of the Raman bands in the O–H stretching region. The fitting procedure using the *Residuals* option of Peakfit Software (Jandel Scientific Software) leads to a good agreement between the fitting curve and experimental data. This region is composed of three Gaussian components for water (see Fig. 4). The first component is generally associated to the O–H vibration in tetrabonded water molecules and was named the 'open' contribution, while the second contribution (named the 'closed' component) corresponds to distorted HB network.[28] The third component, which has not been considered in previous Raman studies of water–disaccharide solutions,[6,29] corresponds to the O–H vibration of free water molecules. Figures 2 and 3 show that the O–H stretching

Table 2. Wavenumber and half width at half maximum (HWHM) of the H–O–H bending mode of water molecules for the 49 wt % solutions at $T = 293$ K

(in cm^{-1})	Pure water	Trehalose–water	Maltose–water	Sucrose–water
ω (Raman)	1636.6 ± 0.2	1635.9 ± 1.2	1636.6 ± 0.5	1636.8 ± 0.3
ω (MD)	1603.8 ± 0.4	1610.3 ± 0.4	1612.5 ± 0.4	1612.5 ± 0.4
HWHM (Raman)	55.7 ± 0.5	45.6 ± 1.0	46.5 ± 1.2	44.4 ± 0.7
HWHM (MD)	40.5 ± 0.4	38.4 ± 0.4	37.6 ± 0.4	37.3 ± 0.4

Data obtained from MD calculations at the same concentrations and $T = 273$ K for the density of states of a flexible water model[26] are also indicated.

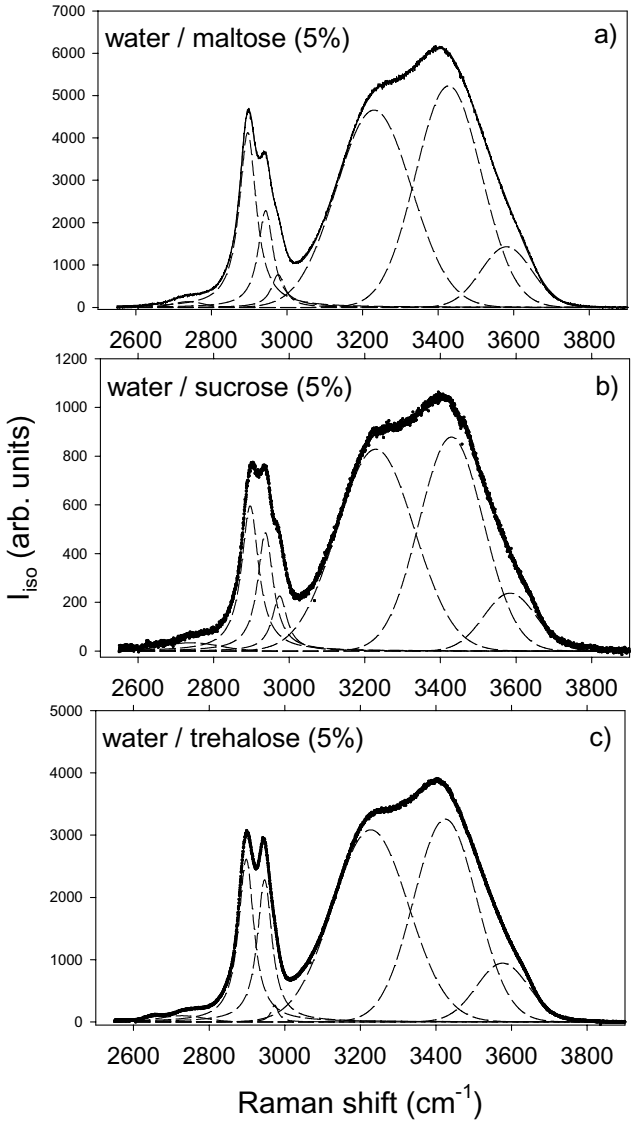

Figure 2. Raman spectra in the C–H and O–H stretching regions of water–disaccharide mixtures with a weight fraction of sugar of 5%. The dashed lines correspond to the components resulting from the fitting procedure.

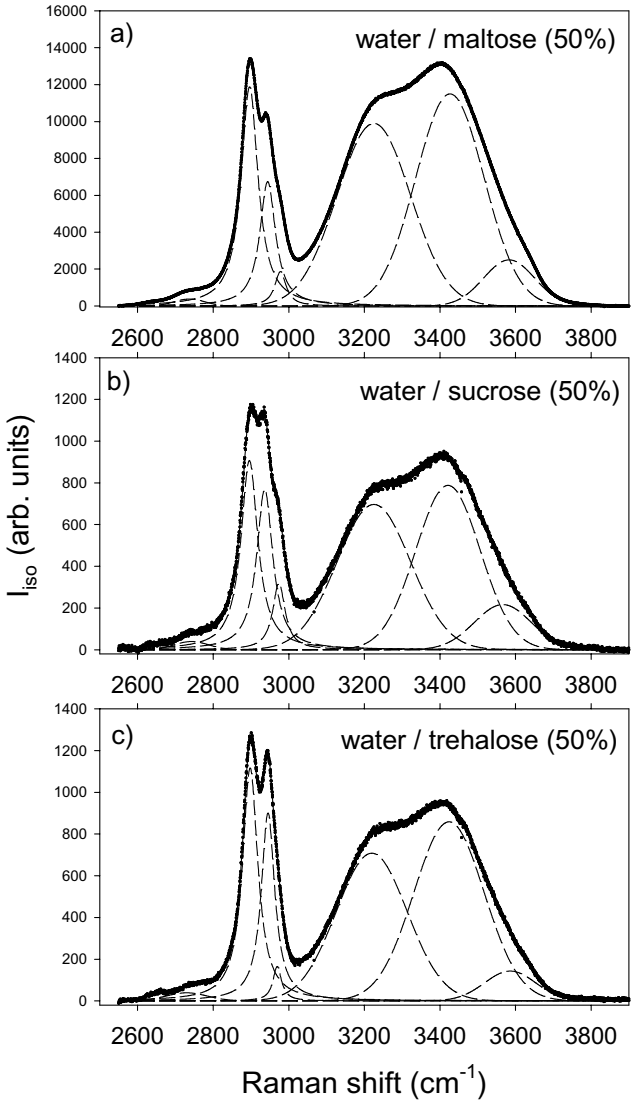

Figure 3. Raman spectra in the C–H and O–H stretching regions of water–disaccharide mixtures with a weight fraction of sugar of 50%. The dashed lines correspond to the components resulting from the fitting procedure.

region of the water–sugar mixtures is composed of these three components. The relative integrated intensity of the ν(OH) stretching bands corresponding to the 'open' component and to the free water molecules with respect to the total intensity of the O–H stretching region is plotted against concentration of sugars for the three sugars (see Fig. 5). It is worth noticing that both O–H stretching bands of water and sugars are detected and overlap in the 2800–3800 cm^{-1} region. Moreover, Fermi resonance between δ(HOH) and ν(OH) may modify the envelope of the O–H stretching band. However, taking into account the very flat line shape of the δ(HOH) bending band and the good agreement between experimental data and the fitting curve (with three Gaussian components), this contribution was not considered.

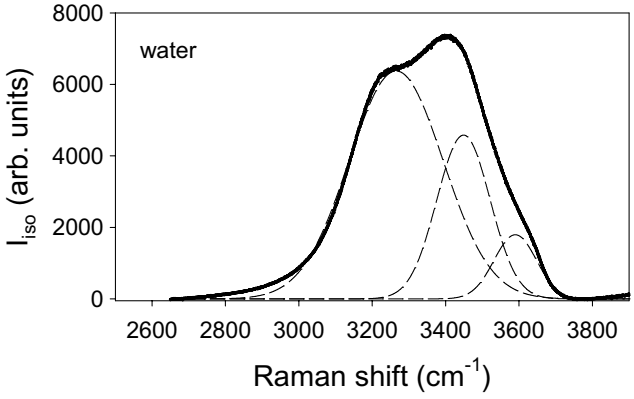

Figure 4. Raman spectra in the O–H stretching region of water. The dashed lines correspond to the components resulting from the fitting procedure.

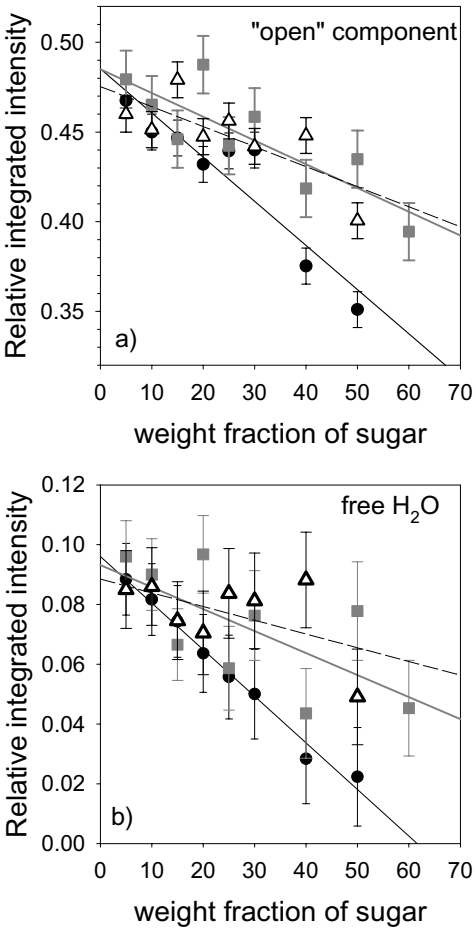

Figure 5. The relative integrated intensity of the first and third O–H stretching bands (with respect to the total intensity of the O–H stretching vibrations) against weight fraction of sugar. Open triangles correspond to maltose, full grey squares to sucrose and full black circles to trehalose. Lines correspond to linear regressions.

Consequently, the relative intensity of the 'open' contribution is not rigorously proportional to a rate of OH groups involved in the tetrabonded H-bond network, with respect to OH groups of water molecules. The same consideration also concerns the 'closed' contribution. Nevertheless, this relation can be considered as a good approximation for low contents of sugar. On the other hand, the intensity of the third component corresponding to the OH groups of free water molecules, can be related to the ratio of free water molecules in sugar aqueous solution, from the consideration of a coefficient representative of the number of OH groups in one water molecule (2) and in one sugar molecule (8). Figure 5 reveals a similar concentration dependence of the relative intensity of each component determined in the O–H stretching region in sucrose, maltose, and trehalose aqueous solutions for low weight fractions of sugar ($\leqslant$30%). Above 30% of sugar, the concentration dependence of intensities in trehalose aqueous solution deviates from those determined in the maltose and sucrose–water mixtures. The decrease of the 'open' band intensity with increasing concentration of sugar in the three sugar aqueous solutions indubitably reveals a destructuring effect of three sugars on the HB network of water as suggested by Magazù and co-workers.[29] 30% Appears as a special content of sugar above which trehalose exhibits a more destructive effect on the H-bond network of water molecules. This result is also confirmed from the decrease of the free water band intensity. It suggests that sugars impose their own HB structure to water, trehalose being the most effective to perform this work. This would mean that trehalose lowers more efficiently the crystallization temperature of biological solutions by disturbing the HBN of water to a larger extent than do sucrose and maltose.

4.2. Statistical distribution of water HB probabilities from MD simulations

The HB network of water may be described by the populations f_j of water molecules that form j HBs with their neighboring water molecules.[30] Indeed, water molecules can be involved in four water–water linear HBs (two as proton donor and two as proton acceptor) in perfect ice, because each one is surrounded by four neighbors which form a perfect tetrahedron. In real water, deviations from this ideal view occur and bifurcated HBs as well as non-H-bonded hydroxyl groups exist.[31] In the present study, two water molecules are considered to be H-bonded if the oxygen–oxygen distance d_{OO} is less than 3.4 Å and the O–H$\cdots$O angle larger than 160°. This geometric criterion has already been used in previous MD studies.[32] The populations f_j of water molecules that form j HBs with their neighboring water molecules for the 66 wt % solutions and for pure water at $T = 293$ K are reported in Table 3. It should be mentioned that f_0 does not correspond to the ratio of free water determined experimentally since it also includes a large number of water molecules bonded to sugar. Addition of disaccharide molecules in the solution leads to a significant increase of f_0 and f_1 and decrease of f_2, f_3, and f_4. It proves that the structure of water is strongly influenced

Table 3. Populations f_j of water molecules forming j HBs with other neighboring water molecules for pure water and the 66 wt % sugar/water solutions

	Pure water	Trehalose–water	Maltose–water	Sucrose–water
f_0	0.068	0.192	0.176	0.178
f_1	0.260	0.414	0.401	0.405
f_2	0.368	0.300	0.307	0.309
f_3	0.237	0.084	0.101	0.095
f_4	0.062	0.008	0.012	0.011
n_H	—	4.598	4.115	4.127

Very small f_5 values have been omitted for clarity. The hydration numbers of the three sugars are also given at this concentration.

by the presence of sugar molecules. Moreover, the tetrahedral HBN of water is more perturbed by the presence of trehalose than with sucrose or maltose as revealed from Table 3. This agrees with the present Raman scattering experimental investigation showing a higher destructuring effect of trehalose. This result appears as a direct consequence of the difference observed on the hydration numbers of the different disaccharides. Indeed, as observed in the present investigations and from different experiments[7,33] and other simulations[12,15,34] trehalose is always found to exhibit the higher hydration number. So it clearly binds to a larger number of water molecules and consequently the water structure will be more affected by this sugar than by the others.

By referring to the concept of intact and broken bonds, it is possible to deduce p_{HB}, the probability of forming an intact bond from the previous distributions. Indeed, assuming that the HB formation is not cooperative[35] and the coordination number in liquid water is 4, the fraction f_j follows the binomial distribution:[30]

$$f_j = \binom{4}{j} \cdot p_{HB}^{j} \cdot (1 - p_{HB})^{4-j}. \quad (1)$$

Figure 6 shows the evolution of p_{HB} as a function of the disaccharide concentration at 293 K obtained from Eq. 1. Similarly to Figure 5, we observe that sugars have a weak influence on the HB probability below a weight fraction of sugar of about 30%. Above this value, confirmed as a threshold in previous MD simulations using a Voroinoi cells analysis,[36] the influence of the three disaccharides can be clearly seen. This figure also shows that trehalose is the most efficient to destructure the water HB network as demonstrated previously. This may again imply that trehalose is the best cryoprotectant among the studied disaccharides.

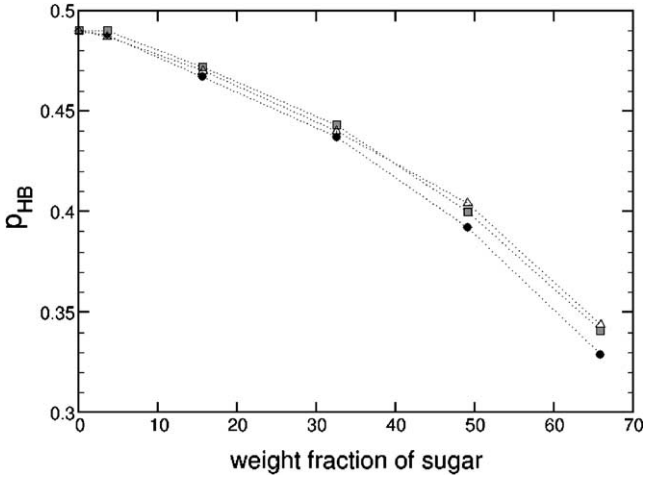

Figure 6. Concentration dependence of the probability of HB formation p_{HB} for the disaccharide solutions at $T = 293$ K. Open triangles correspond to maltose, full grey squares to sucrose and full black circles to trehalose.

5. Conclusion

In the present study, from the analysis of the 'open' contribution in the O–H stretching region, it is clearly observed that trehalose possesses a superior destructuring effect on the H-bond network of water for sugar weight fractions above 30%. Below this concentration, sugars behave similarly. This new result is confirmed from MD calculations of the statistical distribution of water HB probabilities. MD computations also suggest that the hydration number of the different sugars could be a pertinent parameter in order to explain why trehalose exhibits this higher destructuring effect. The contribution of the O–H stretching vibration corresponding to free water molecules, determined for the first time in sugar aqueous solutions, is consistent with this result. This may suggest that trehalose is the best cryoprotectant among the studied disaccharides, because it modifies to a larger extent than do maltose or sucrose the HBN of water, and thus, lowers more significantly the temperature of crystallization of biological solutions. The findings obtained on the bending mode of water indicate the presence of smaller and more homogeneous domains of water molecules but no clear difference between trehalose, sucrose and maltose can be seen. Finally, the conformational changes of sugars, which may occur when increasing concentration, should influence the vibrational properties of water molecules. Therefore, the study of the intramolecular vibrations of sugars in the [700–1400] cm^{-1} frequency range will be undertaken in a next study.

Acknowledgements

The authors wish to acknowledge the use of the facilities of the IDRIS (Orsay, France) and the CRI (Villeneuve d'Ascq, France) where calculations were carried out. This work was supported by the INTERREG III (FEDER) program (Nord Pas de Calais/Kent).

References

1. *Biophysics and Biochemistry at Low Temperatures*; Franks, F., Ed.; Cambridge University Press: Cambridge, 1985.
2. Crowe, J. H.; Leslie, S. B.; Crowe, L. M. *Cryobiology* **1994**, *31*, 355.
3. Green, J. L.; Angell, C. A. *J. Phys. Chem.* **1989**, *93*, 2880.
4. Taylor, L. S.; Zografi, G. D. *J. Pharm. Sci.* **1998**, *87*, 1615.
5. Miller, D. P.; de Pablo, J. J. *J. Phys. Chem. B* **2000**, *104*, 8876.
6. Branca, C.; Magazù, S.; Maisano, G.; Migliardo, P. *J. Phys. Chem. B* **1999**, *103*, 1347.
7. Branca, C.; Magazù, S.; Maisano, G.; Migliardo, F.; Migliardo, P.; Romeo, G. *J. Phys. Chem. B* **2001**, *105*, 10140.

8. Sussich, F.; Skopec, C.; Brady, J.; Cesàro, A. *Carbohydr. Res.* **2001**, *334*, 165.
9. Akao, K.; Okubo, Y.; Asakawa, N.; Inoue, Y.; Sakurai, M. *Carbohydr. Res.* **2001**, *334*, 233.
10. Nagase, H.; Endo, T.; Ueda, H.; Nakagaki, M. *Carbohydr. Res.* **2002**, *337*, 167.
11. Crowe, J. H.; Crowe, L. M.; Oliver, A. E.; Tsvetkova, N.; Wolkers, W.; Tablin, F. *Cryobiology* **2001**, *43*, 89–105.
12. Brady, J. W.; Schmidt, R. K. *J. Phys. Chem.* **1993**, *97*, 958.
13. Engelsen, S. B.; du Penhoat, C. H.; Pérez, S. *J. Phys. Chem.* **1995**, *99*, 13334.
14. Liu, Q.; Schmidt, R. K.; Teo, B.; Karplus, P. A.; Brady, J. W. *J. Am. Chem. Soc.* **1997**, *119*, 7851.
15. Conrad, P. B.; de Pablo, J. J. *J. Phys. Chem. A* **1999**, *103*, 4049.
16. Ekdawi-Sever, N.; Conrad, P. B.; de Pablo, J. J. *J. Phys. Chem. A* **2001**, *105*, 734.
17. Cottone, G.; Cordone, L.; Ciccotti, G. *Biophys. J.* **2001**, *80*, 931.
18. Cicerone, M. T.; Soles, C. L. *Biophys. J.* **2004**, *86*, 3836.
19. Smith, W.; Forester, T. R. The DLPOLY user manual, CCLRC, Daresbury Laboratory , Warrington WA4 4AD, England (2001).
20. Taga, T.; Senma, M.; Osaki, K. *Acta Cryst. B* **1972**, *28*, 3258.
21. Gress, M. E.; Jeffrey, G. A. *Acta Cryst. B* **1977**, *33*, 2490.
22. Brown, G. M.; Levy, H. A. *Acta Cryst. B* **1973**, *29*, 790.
23. Neumann, M. *J. Chem. Phys.* **1985**, *82*, 5663.
24. Ha, S. N.; Giammona, A.; Field, M.; Brady, J. W. *Carbohydr. Res.* **1988**, *180*, 207.
25. Berendsen, H. J. C.; Grigera, J. R.; Straatsma, T. P. *J. Phys. Chem.* **1987**, *91*, 6269.
26. Teleman, O.; Jönsson, B.; Engström, S. *Mol. Phys.* **1987**, *60*, 193–203.
27. Maréchal, Y. *J. Mol. Struct.* **1994**, *105*, 322.
28. d'Arrigo, G.; Maisano, G.; Mallamace, F.; Migliardo, P.; Wanderlingh, F. *J. Chem. Phys.* **1981**, *75*, 4264.
29. Branca, C.; Magazù, S.; Maisano, G.; Migliardo, P. *J. Chem. Phys.* **1999**, *111*, 281.
30. Stanley, H. E.; Teixeira, J. *J. Chem. Phys.* **1980**, *73*, 3404.
31. Giguère, P. A. *J. Chem. Phys.* **1987**, *87*, 4835.
32. Roberts, C. J.; Debenedetti, P. G. *J. Phys. Chem. B* **1999**, *103*, 7308.
33. Furuki, T. *Carbohydr. Res.* **2002**, *337*, 441.
34. Engelsen, S. B.; Pérez, S. *J. Phys. Chem. B* **2000**, *104*, 9301.
35. Luzar, A.; Chandler, D. *Phys. Rev. Lett.* **1996**, *76*, 928.
36. Bordat, P.; Lerbret, A.; Affouard, F.; Demaret, J.-Ph.; Descamps, M. *Europhys. Lett.* **2004**, *65*(1), 41–47.